RESEARCH

Role of DWI in evaluation of HCC after radiofrequency ablation compared to dynamic MRI using MRI (3 T)

Bahaa Mohamed Elrefaey Hasan[1*] ⓘ, Hanaa Abd ElKader Abd ElHamid[2], Nivan Hany Khater[2], Waseem ElGendy[1] and Ahmed S. Abdelrahman[2]

Abstract

Background: The purpose of this study was to investigate the diagnostic performance of diffusion weight imaging (DWI), apparent diffusion coefficient (ADC) map, normalized ADC liver, and normalized ADC spleen compared to the dynamic contrast-enhanced MRI (DCE-MRI) in the evaluation of residual hepatocellular carcinoma (HCC) after radiofrequency ablation (RFA) using 3 T (T) magnetic resonance imaging (MRI).

Results: A prospective study was performed on 40 patients with radiofrequency-ablated HCC, and 15 (37.5%) patients had viable lesion post-RFA, while 25 (62.5%) had non-viable lesions. DCE-MRI had a sensitivity, specificity, and accuracy of 100%, 100%, and 100%, respectively, compared to DWI which had a sensitivity, specificity, and accuracy of 80%, 88%, and 85%, respectively, for identifying post-RFA viable HCC. The sensitivity, specificity, and accuracy of ADC at a cutoff value of 1.01×10^{-3} mm^2/s were 80%, 100%, and 97.1%, respectively. The optimal cutoff value of normalized ADC liver was 0.81 with a sensitivity of 73.3%, specificity of 96%, and accuracy of 92.8%. The sensitivity, specificity, and accuracy of normalized ADC spleen at a cutoff value of 1.22 were 80%, 92%, and 91.1%, respectively.

Conclusions: DWI-MRI is a reliable technique for assessing HCC after radiofrequency ablation. DWI-MRI with ADC may be used as an alternate sequence for assessing radiofrequency-ablated lesions in individuals who have a contraindication to the contrast media, and the normalized ADC value may be of additional benefit.

Keywords: RFA, HCC, DCE-MRI, DWI, ADC, Normalized ADC, LI-RADS

Background

Hepatocellular carcinoma (HCC) is one of the most global common cancers which has a poor prognosis except if treated. Generally, surgical excision is the standard treatment option for HCC. Another therapeutic option is liver transplantation, which was the best therapeutic option for HCC theoretically. Nowadays, ablative treatments are an alternative therapeutic choice for patients with liver tumors who are not fit for surgery. Thermal ablation is done by using cold (cryoablation) or heat (radiofrequency ablation, laser ablation, and microwave ablation). Radiofrequency ablation (RFA) is one of the most extensively used ablative techniques for the treatment of hepatic primary and secondary tumors, but all hyperthermal techniques cause coagulation necrosis and show identical imaging features in follow-up studies [1]. Radiological imaging is important for guiding RFA procedures and for precise treatment adequacy evaluation and follow-up [2].

Conventional magnetic resonance imaging (MRI) cannot provide exact information about the features of the tissues after RFA therapy as the post-treatment granulation tissue may look like that of a viable tumor, hindering early detection of residual or recurrent tumor after RFA [3]. Dynamic contrast-enhanced magnetic resonance

*Correspondence: bahaaelrefaey@yahoo.com
[1] Radiology Department, Military Medical Academy, Cairo, Egypt
Full list of author information is available at the end of the article

Elrefaey Hasan *et al. Egypt J Radiol Nucl Med*   (2021) 52:267

Page 2 of 12

imaging (DCE-MRI) is the imaging gold standard modality that provides precise qualitative and quantitative data via its multi-parametric capabilities [4].

Diffusion-weighted imaging (DWI) is one of the functional imaging techniques which detect the microscopic changes of the tumor by evaluating the diffusion of water molecules which is restricted in residual or recurrent malignant tissue, allowing early tumor response evaluation after loco-regional therapy [5]. Studies in both animals and humans have revealed that an effective tumor treatment produces an increase in the apparent diffusion coefficient (ADC) value, which can occur before any measurable change in tumor size [6].

By using recently available machines, DWI can be added easily to the routine examination. This imaging method has a high capability for hepatic focal lesion (HFL) detection, and quantitative evaluation can be achieved without contrast media. Also, it is suitable for patients who suffer from contrast media allergy or renal dysfunction [7].

The aim of this study was to evaluate the diagnostic performance of DWI, ADC, and normalized ADC in the assessment of viable HCC following radiofrequency ablation as compared to the dynamic contrast-enhanced MRI using 3 T (T) MRI.

Methods

Patients

This prospective study was carried out at our institution after the approval of our ethical committee. All participants in this study provided informed consent. This study at first included 50 patients, 5 patients were excluded due to raised serum creatinine, 3 patients were excluded due to having cardiac pace maker, 2 patients were excluded due to having a claustrophobia, and finally, 40 patients were included in our study. Patients suffering from HCC secondary to viral hepatitis and who underwent RFA were included in this study during the period from April 2019 till March 2021, and patients with equivocal and non-evaluable Liver Imaging Reporting and Data System treatment response (LR-TR) were omitted from the current investigation. Also, patients with a contraindication to MRI, i.e., metallic clips of an aneurysm and cardiac pacemaker, who are suffering from claustrophobia and who have a contraindication to the contrast media were excluded from this study.

All patients came in for follow-up by DCE-MRI with diffusion-weighted images in about 3 months following RFA treatment to observe tumoral post-treatment response, and then, follow-up after another 3 months later was done for non-viable, equivocal, and non-evaluable post-treatment response categories, while for LR-TR viable lesions another follow-up done before the second session of RFA.

Technique of DCE-MRI examination

The MRI was performed with a 3 T MRI (General Electric scanner, Healthcare, America) using a 32-channel phased-array coil. A respiratory belt was wrapped across the patient's abdomen to aid in breath synchronization. Field of view: $35 \times 28 \times 22$ cm. Matrix: 320×192. Slice thickness 7 mm, gap: 1 mm. Sequences: Axial T2 WI single shot spine echo (TR/TE: 7200/110 ms), Breath-hold coronal single-shot T2-WI turbo spin-echo (TSE) (TR/TE: 704/310 ms, 90° flip angle). In-phase axial T1-weighted gradient echo (TR/TE: 15/5 ms), out-of-phase axial T1-weighted gradient echo (TR/TE:10/2.2 ms, 15° flip angle), and respiratory-triggered axial DWI (echo-planar imaging (EPI); b values, 0, 500 and 800 s/mm^2; TR/TE: 2300/63 ms, 80 EPI factor, 5 mm slice thickness, 1 mm gap, 90° flip angle, 2 acceleration factor). Dynamic multi-phase 3D liver acquisition with volume acceleration (LAVA) T1-weighted sequence was performed (arterial, 10–20 s; late arterial, 30–40 s; portal/venous, 60–90 s; and delayed, 180–210 s) after injection of 10–15 ml gadolinium contrast media at a rate of 2 ml/s (TR/TE: 3.8/1.8 ms, 12° flip angle, and slice thickness: 2–3 mm).

Analysis of data

Imaging analysis

A dynamic contrast-enhanced MRI study was reported independently by two experienced radiologists (11 and 8 years of experience in abdominal imaging) using a secondary workstation (Discovery 750) according to the Liver Imaging Reporting and Data System (LI-RADS) v2018 lexicon [8]: LR-TR non-viable for a lesion with no enhancement in the DCE-MRI or a lesion expressing the expected treatment-specific enhancement pattern and LR-TR viable post-ablated HCC for residual enhancing nodular or thick irregular tissue with one or more of the following characteristics: arterial phase

---

(See figure on next page.)

Fig. 1 Male patient 56 years old with chronic viral hepatitis C and HCC in segment VII diagnosed as HCC. He underwent RFA; follow-up MRI was done after 13 weeks after ablation revealed a high ADC value and no diffusion restriction in a non-viable ablated bed. The lesion showed a low signal at T1WI (**a**), a high signal at T2WI (**b**), it shows no contrast enhancement at DCE series "arterial (**c**), portal (**d**), delayed (**e**) phases", and the lesion showed a low signal at DWI b value = 800 (**f**) and corresponding high signal at ADC mapping series (**g**, **h**) ADC = 2.1×10^{-3} mm^2/s

Elrefaey Hasan *et al. Egypt J Radiol Nucl Med*   (2021) 52:267

Page 3 of 12

Fig. 1 (See legend on previous page.)
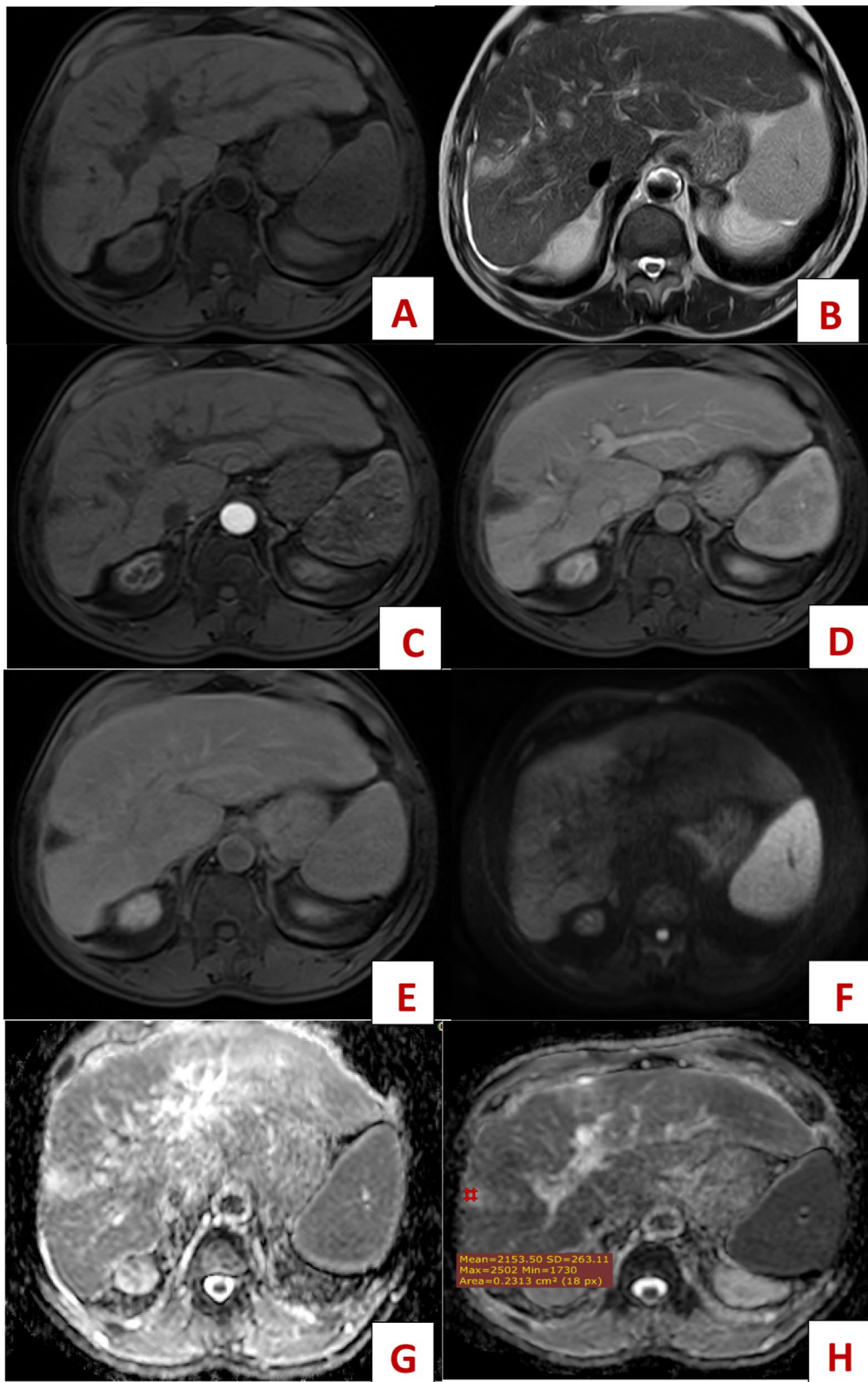
Elrefaey Hasan *et al. Egypt J Radiol Nucl Med*   (2021) 52:267

Page 4 of 12

hyperenhancement, washout, or enhancement equivalent to pretreatment HCC. The size and the signal intensity of the lesions were also evaluated. In situations where there was disagreement between the two radiologists, a definitive diagnosis was obtained by consensus.

Using Discovery software version 26.1, the DWI and ADC map was analyzed blindly and independently by two experienced radiologists (with 10 and 9 years of experience) and the definitive diagnosis was made by consensus. A viable HCC was diagnosed if the lesion expressed a bright signal in the DWI with *b* value of 800 s/mm^2 and a low signal in the corresponding ADC map; otherwise, the HCC was diagnosed. On the other hand, the ADC values were measured three times and the mean was calculated. The region of interest (ROI) was drawn manually in the whole area with restricted diffusion if the lesion had diffuse homogeneous or heterogeneous signal in the ADC map. However, if the lesion had well-defined areas of facilitation and other areas of restriction, the ROI was drawn on each area with restricted diffusion and their ADC values were calculated separately.

The ratio of the hepatic lesion ADC to the surrounding liver parenchyma ADC (normalized ADC liver) and the splenic parenchyma ADC (normalized ADC spleen) was used to procure the normalized ADC values (nADC) of the hepatic lesion.

All patient included at our study had already HCC which was diagnosed and come for follow-up. Histopathology reports were difficult to get since surgery was not an appropriate therapeutic option in our cases, and there were also biopsy collection mistakes owing to technical problems. Follow-up at our study was done by DCE-MRI/DWI after 3 months after RFA and repeated for ensuring the results; for the viable/recurrent lesion, the follow-up was done before the second session of RFA. The LI-RADS v2018 criteria were utilized to evaluate the responsiveness of post-RFA therapy. So, our standard of reference was LR-TR viable category (residual/recurrent HCC) for treated lesions with non-rim peripheral APHE and/or delayed washout in DCE-MRI follow-up imaging (Figs. 3 and 4), LR-TR non-viable (resolved lesions) for treated hepatic lesions with no pathological arterial enhancement (Figs. 1 and 2), LR-TR non-evaluable category for cases with image degradation due to motion artifacts, and LR-TR (equivocal) for atypical enhancement not expected for treatment-specific expected post-contrast enhancement pattern and also not meeting criteria for viability. Diffusion restriction promotes reader confidence hand in hand with positive dynamic imaging findings.

Statistical analysis

The data were coded and fed to statistical software SPSS (Statistical Package for the Social Sciences) version 25 and summarized using mean, standard deviation, median, minimum, and maximum in quantitative data and frequency percentage in categorical data. The specificity, sensitivity, positive predictive value (PPV), negative predictive value (NPV), and accuracy were computed for categorical data. The optimal ADC cutoff value was determined using receiver operating characteristic (ROC) curves and the area under the curve analysis. The parametric *T* test was used to make comparisons between quantitative variables. The Chi-square (χ^2) test was used to compare categorical data. When the predicted frequency is less than 5, an exact test was employed instead. *P* value less than 0.05 was considered statistically significant. The power of sample size calculation was 85%.

Results

This prospective study included 40 individuals with radiofrequency-ablated HCC: 30 men (75%) and 10 females (25%). The mean age of all patients was 58.95 ± 7.43 years (age range 44–75 years).

As indicated in Table 1, 15 (37.5%) of the 40 HCC treated lesions revealed the radiological appearance of LR-TR viable post-treatment response; 4/15 showed solely arterial phase hyperenhancement and 11/15 displayed arterial phase hyperenhancement with washout, whereas there were no enhancements in the remaining 25 (62.5%) lesions that were judged as LR-TR non-viable ablated bed. The mean size of the viable lesions was statistically similar to the non-viable ablated bed (34.4 ± 12.99 mm versus 30.6 ± 8.09 mm, respectively, $P = 0.260$), and the size range of all lesions was from 20 to 68 mm.

Regarding the T1 WI signal intensity of the ablated lesions, the majority of the lesions expressed isointense signal (40%), followed by hypointense (27.5%),

(See figure on next page.)

Fig. 2 Male patient 43 years old with chronic viral hepatitis C and HCC in segment VIII diagnosed as HCC. He underwent RFA; follow-up MRI study was done after 12 weeks after ablation revealed high ADC value and no diffusion restriction in a non-viable ablated bed. The lesion showed an isointense signal at T1WI (**a**), hypointense signal at T2WI (**b**), at DCE-MRI "arterial (**c**), portal (**d**) and delayed (**e**) series" showed no significant enhancement, DWI at *b* value 500 (**f**) and 800 (**g**) showed no restricted diffusion, with a corresponding high signal at ADC series (**h**) (ADC value $= 1.35 \times 10^{-3}$ mm^2/s)
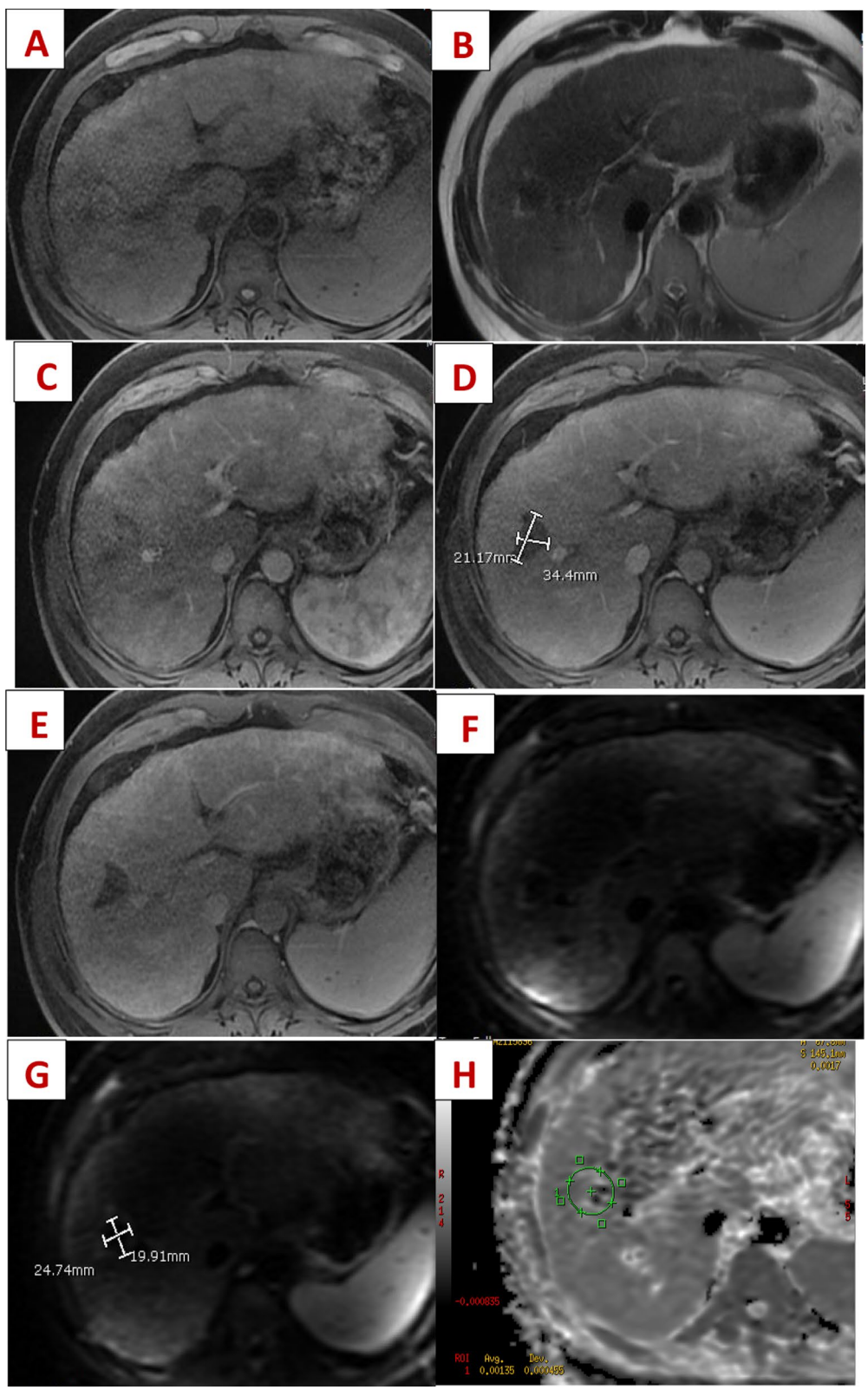
Elrefaey Hasan *et al. Egypt J Radiol Nucl Med*   (2021) 52:267

Page 5 of 12

Fig. 2 (See legend on previous page.)

Elrefaey Hasan *et al. Egypt J Radiol Nucl Med*   (2021) 52:267

Page 6 of 12

Table 1 Size and enhancement of the radiofrequency-ablated HCC

	Viable (15)	Non-viable (25)	Test	P value
Mean lesion size ± SD (mm)	34.4 ± 12.99	30.6 ± 8.09	− 1.144[a]	0.260[+]
Lesion size range (mm)	20–68	20–48		
Enhancing lesion	15	0	40.00[b]	< 0.001*
Arterial phase hyperenhancement	15	0		
Washout	4	0		

*Significant

[+] Non-significant

[a] *T* test

[b] (x^2) Chi-square test

Table 2 T1 WI and T2 WI signals of radiofrequency-ablated HCC

	Total	Viable	Non-viable	X^{2+}	P value
T1 WI				12.56	0.006*
Hypo	11 (27.5%)	8 (53.3%)	3 (12%)		
Iso	16 (40%)	6 (40%)	10 (40%)		
Inter	2 (5%)	1 (6.7%)	1 (4%)		
Hyper	11 (27.5%)	0	11 (44%)		
T2 WI				10.74	0.005*
Hypo	12 (30%)	0	12 (48%)		
Iso	7 (17.5%)	3 (20%)	4 (16%)		
Hyper	21 (52.5%)	12 (80%)	9 (36%)		

*Significant

[+] (X^2) Chi-square

Table 3 ADC values among viable and non-viable post-RFA HCC

	Viable	Non-viable	T test	P value
ADC value ($\times 10^{-3}$ mm²/s)				
Mean ± SD	0.965 ± 0.128	1.330 ± 0.222	5.790	< 0.001*
Range	0.85–1.23	1.02–2.1		
nADC liver				
Mean ± SD	0.743 ± 0.094	0.980 ± 0.172	4.890	< 0.001*
Range	0.62–0.89	0.81–1.4		
nADC spleen				
Mean ± SD	1.113 ± 0.191	1.518 ± 0.268	5.104	< 0.001*
Range	0.87–1.56	1.16–2.4		
Liver ADC ($\times 10^{-3}$ mm²/s)				
Mean ± SD	1.285 ± 0.119	1.360 ± 0.124	1.891	0.066
Range	1.04–1.49	1.1–1.57		
Spleen ADC ($\times 10^{-3}$ mm²/s)				
Mean ± SD	0.869 ± 0.121	0.886 ± 0.109	0.449	0.656
Range	0.55–1.02	0.68–1.1		

nADC normalized ADC

*Significant

[+] Non-significant

hyperintense (27.5%), and finally by intermediate intensity (5%). While the most frequent T1 WI signal intensity seen in the viable lesion was hypointensity (8/15) and isointensity (6/15), the hyperintensity (11/25) and isointensity (10/25) were the most noticeable T1 WI signals in the non-viable ablated bed (*P* = 0.006). On the other hand, hyperintensity (52.5%) and hypointensity (30%) were the most frequently observed T2 WI signal in the ablated bed; however, the majority of the non-viable ablated bed exhibited T2 WI hypointense (12/25) and hyperintense (9/25) signal, while the hyperintense signal (12/15) was the most frequently observed T2 WI signal in the viable lesion (*P* = 0.005) (Table 2).

The mean ADC value of viable tumors was statistically significantly lower than that of non-viable tumors ($0.965 \pm 0.128 \times 10^{-3}$ mm²/s vs. $1.330 \pm 0.222 \times 10^{-3}$ mm²/s, respectively, *P* value < 0.001), and the mean value of normalized ADC liver and normalized ADC spleen was also significantly lower in the viable tumors (0.743 ± 0.094 and 1.113 ± 0.191, respectively) than in the non-viable tumors (0.980 ± 0.172 and 1.518 ± 0.268,

(See figure on next page.)

Fig. 3 Male patient 64 years old with HCC in segment VII underwent RFA 8 months ago, MRI study was done after 14 weeks after ablation, and it revealed low ADC value and diffusion restriction in a viable lesion. The lesion showed a low signal at T1WI (**a**), a high signal at T2WI (**b**); at the DCE series the lesion showed peripheral thick arterial phase hyperenhancement (**c**) and gradual washout at portal phase (**d**) and delayed phase (**e**), while the center of the lesion showed no enhancement at all DCE phases; DWI b 500 (**f**) and b 800 (**i**) showed marginal thick restricted diffusion, with low signal at ADC mapping series (**g**, **h**) at its margin (ADC value = 0.98×10^{-3} mm²/s) and bright signal at its center (ADC value = 2.4×10^{-3} mm²/s)

Elrefaey Hasan *et al. Egypt J Radiol Nucl Med*   (2021) 52:267
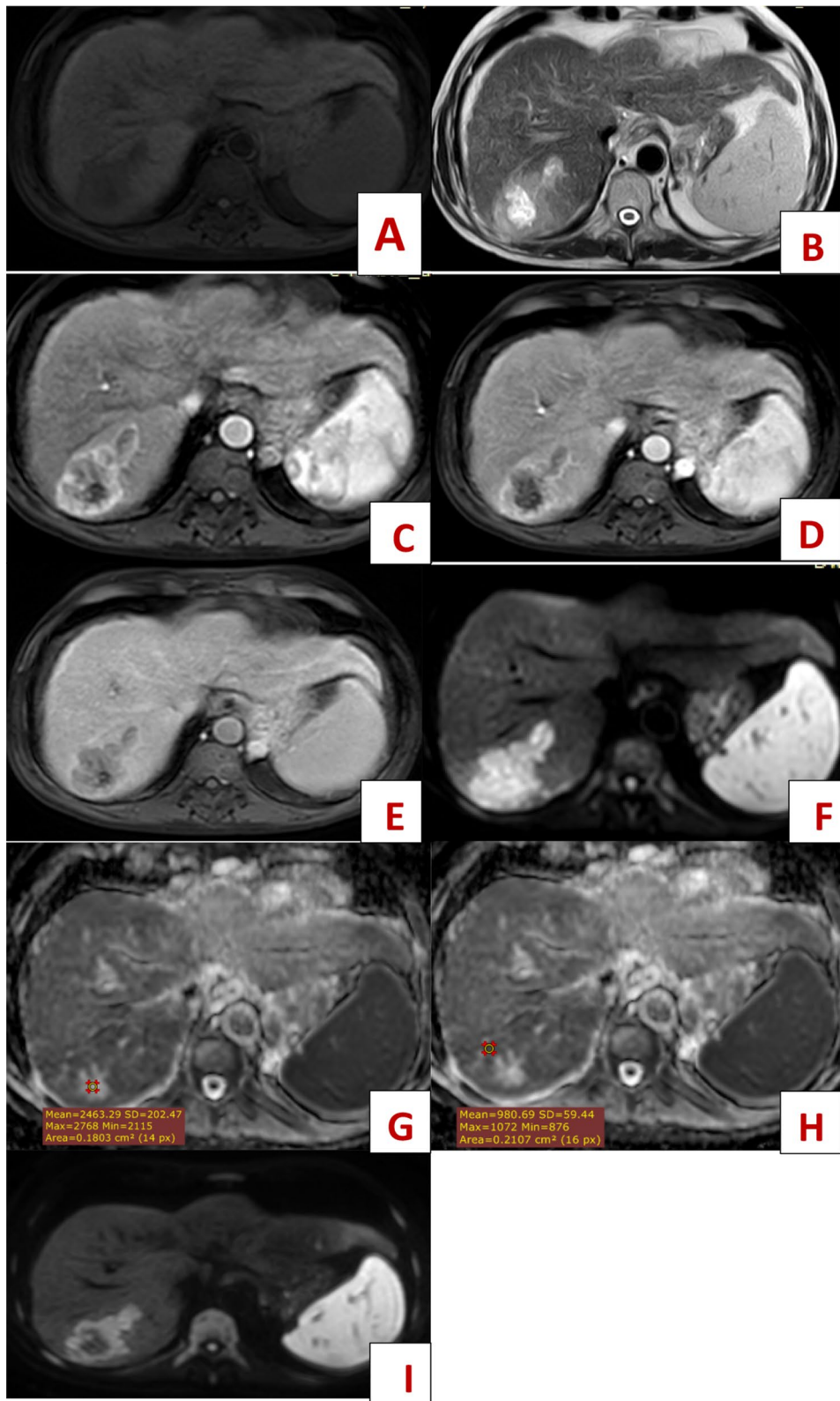
Page 7 of 12

Fig. 3 (See legend on previous page.)

respectively). In both viable and non-viable tumors, however, there was no significant difference in the mean ADC value of the liver and spleen ($P = 0.066$ and 0.656, respectively) (Table 3).

The optimal cutoff value of the ADC for distinguishing viable from non-viable HCC following RFA was 1.01×10^{-3} mm^2/s (Fig. 5) with sensitivity, specificity, and accuracy of 80%, 100%, and 97.1%, respectively. The optimum cutoff values for the normalized ADC liver and normalized ADC spleen (Fig. 5), on the other hand, were 0.81 and 1.22, respectively, with sensitivity of 73.3% and 80%, specificity of 96% and 92%, and accuracy of 92.8% and 91.9%, respectively (Figs. 1, 2, 3, 4 and 5). The DWI had a similar sensitivity of 80% but relatively lower specificity and accuracy of 88% and 85%, respectively. On the other hand, DCE-MRI had a different statistical values as sensitivity 100%, specificity 100%, and accuracy 100% (Table 4).

The matched cases between both observers for DCE-MRI positive and negative results were 15/15 (100%) and 24/25 (96%), respectively, and an almost perfect inter-reader agreement was noted ($K = 0.947$, $P < 0.001$), while the matched cases between both observers for DWI positive and negative results were 14/15 (93.33%) and 24/25 (96%), respectively, and an almost perfect inter-reader agreement was noted ($K = 0.893$, $P < 0.001$).

Discussion

Hepatocellular carcinoma is the most common hepatic primary malignant tumors and is the third leading cause of cancer deaths worldwide. It claims the lives of around 500,000 people every year [9]. Functional MRI techniques as diffusion-weighted imaging detect early MR signal changes in tissues within several weeks after RFA, based on the degree of cell membrane integrity [10].

The purpose of this study was to evaluate the clinical utility of DWI compared to the dynamic contrast-enhanced MRI using a 3 T MRI unit in detecting remaining viable tissue in HCC following radiofrequency ablation.

The current study, like other studies [11–13], found overlap in the T1 WI and T2 WI signal intensity between the non-viable well-ablated bed and the viable lesion where the T2 WI hyperintensity was noted in 80% of the viable lesion and 36% of the non-viable ablated bed. Coagulation necrosis, hemorrhage, and the residual viable lesion are responsible for this considerable heterogeneity in the signal intensities which may complicate the assessment of HFL

after RFA [11]. On the other hand, the hyperintense signal was the most detected T1 signal in the non-viable ablated bed and the hypointense signal was the most frequently noted signal in the viable lesion, yet 40% of both viable and non-viable ablated bed exhibited isointense signal. When evaluating the post-treatment response to RFA utilizing abbreviated MRI procedures, this overlap in signal intensity raises debate, and future research may emphasize the advantage of the non-contrast MRI sequence.

In this study, a DWI with satisfactory imaging quality and reasonable acquisition duration was achieved utilizing parallel imaging and the breath-hold methods on a 3-T scanner with b values of 0, 500, and 800 s/mm. Saleh et al. [13] utilized 3 T MRI equipment with similar b values, while Ebeed et al. [12] used a 1.5 T MRI unit with b values of 50, 400, and 800 s/mm^2.

In the present study, 15 patients had lesion enhancement that was classified as a viable lesion following RFA, and Chernyak et al. [14] state that the presence of either arterial phase hyperenhancement or washout, independent of lesion size, is sufficient to define a treated lesion as viable.

In the current study, the sensitivity and specificity of DWI were 80% and 88%, respectively, and a similar result was also obtained in a study done by Ludwig et al. [15] who revealed that the sensitivity and specificity of DWI for diagnosing viable HCC after loco-regional therapy were 78.6% and 88.4%, respectively, yet Youssef et al. [16] revealed lower specificity after loco-regional treatment for HCC with a specificity value of 64.3%. The DWI falsely diagnosed three non-viable ablated beds as viable with diffusion restriction noted, which was related to the post-ablation tumoral necrosis and hemorrhage. Hypercellularity mixed with a fibrotic component in the peri-lesion parenchymal inflammatory granulation would limit water diffusion [17].

The mean ADC value of the viable lesions in our study was statistically significantly lower than that of the non-viable lesion ($P < 0.001$), and the best ADC cutoff value for discrimination between viable and non-viable ablated bed post-RFA was 1.01×10^3 mm^2/s with sensitivity of 80% and specificity of 100%, and other studies which evaluated the ADC after RFA showed higher cutoff values with a range from 1.05 to 1.19×10^{-3} mm^2/s [18–20]. These studies were conducted in a 1.5 T MRI unit, yet in the current study, a 3 T MRI unit was used which provide a higher signal-to-noise ratio and better DWI resolution.

(See figure on next page.)
Fig. 4 Female patient 49 years old with HCC at segment VII underwent RFA. MRI study was done after 13 weeks after ablation and revealed low ADC value and diffusion restriction in a viable lesion. The lesion showed an intermediate signal at T1WI (**a**), an isointense signal at T2WI (**b**); at DCE series showed arterial phase hyperenhancement (**c**) and gradual washout at portal phase (**d**) and delayed phase (**e**), restricted diffusion seen at DWI at *b* value 500 (**f**) and 800 (**g**), with corresponding low signal at ADC series (H) ADC value $= 0.92 \times 10^{-3}$ mm^2/s
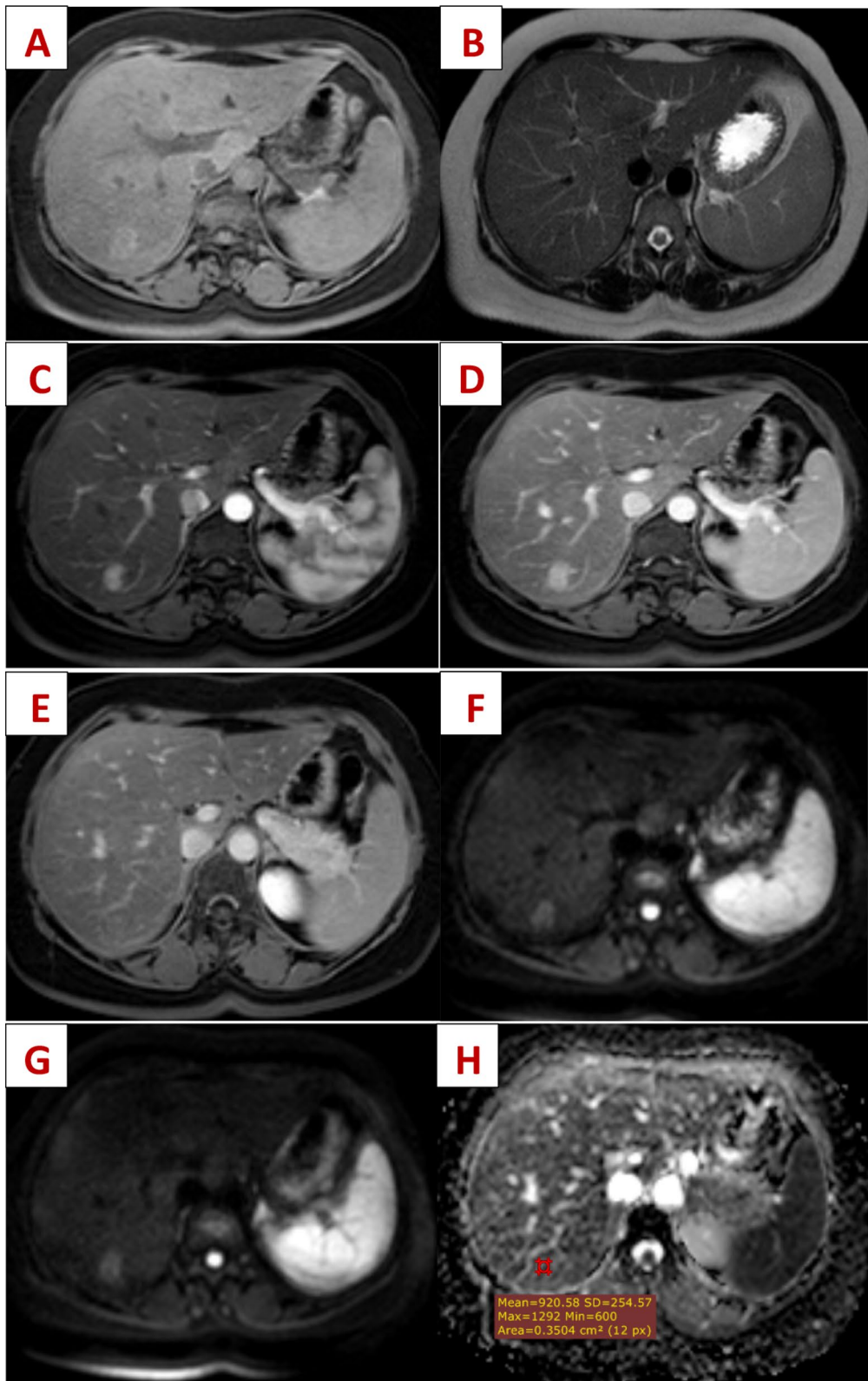
Elrefaey Hasan *et al. Egypt J Radiol Nucl Med*   (2021) 52:267

Page 9 of 12

Fig. 4 (See legend on previous page.)

Elrefaey Hasan *et al. Egypt J Radiol Nucl Med*   (2021) 52:267
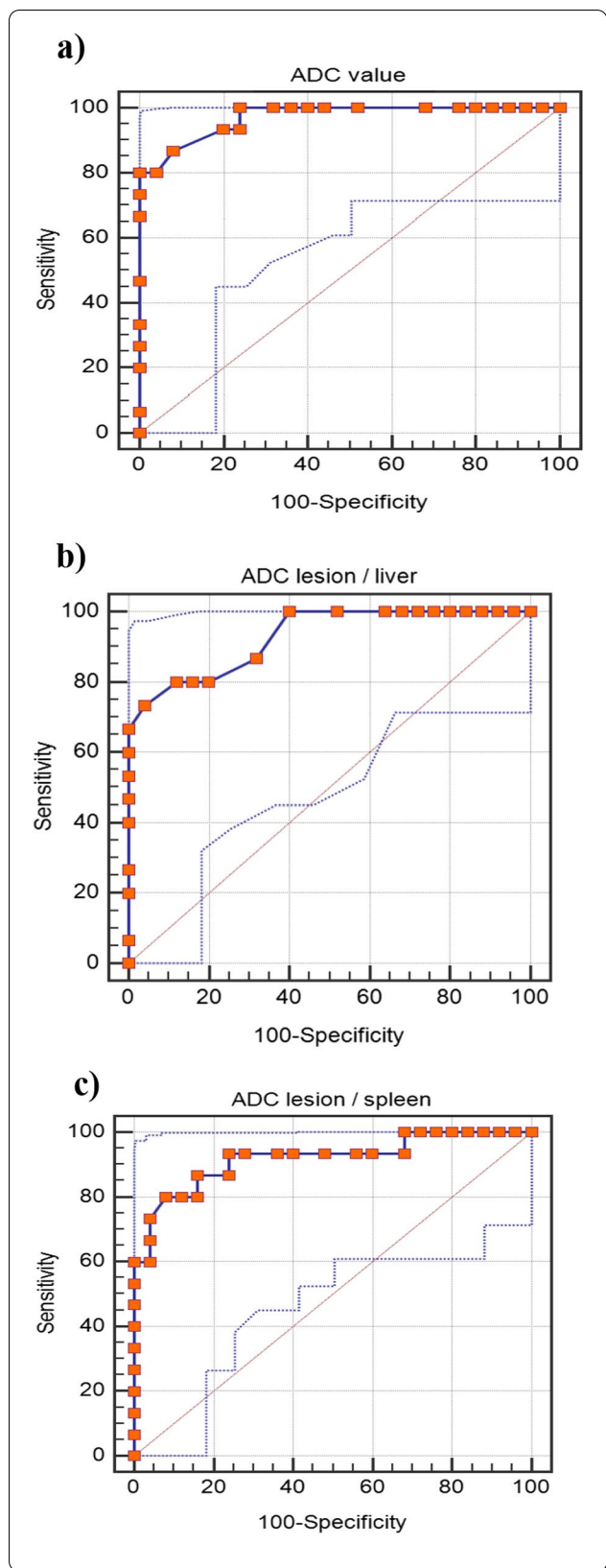
Page 10 of 12

Fig. 5 a Receiver operating characteristic (ROC) curve of ADC. **b** Receiver operating characteristic (ROC) curve of normalized ADC liver. **c** Receiver operating characteristic (ROC) curve of normalized ADC spleen

The normalized ADC liver and normalized ADC spleen were used to differentiate between non-viable and viable lesions in the current study, and to our knowledge, no previous study had used these normalized ADC values. However, a study was done on the pancreas to differentiate between benign and malignant lesions, which revealed a statistically significant difference in the mean normalized ADC values between the benign and malignant lesions [21].

In our study, we reported that the normalized ADC liver cutoff value was 0.81 with a sensitivity of 73.3% and specificity of 96%, while the normalized ADC spleen cutoff value was 1.22 with a sensitivity of 80% and specificity of 92%. Although the sensitivity and specificity of ADC were greater than that of normalized value, both were comparable and further research may reveal the added usefulness of this new measurement.

The standardized reporting technique must be a dynamic process that is subject to clinical and radiological reassessment as well as data validation in order to be evaluated and developed further [22–24]. The DWI was regarded as one of the minor characteristics in the LI-RADS v2018 for categorization of the non-treated hepatic focal lesion, while the LI-RADS treatment response is based solely on the enhanced pattern of the treated HCC, and it does not include the DWI and ADC. Many previous trials, including this study, have shown the usefulness of DWI and ADC in detecting residual HCC following loco-regional treatment. The DWI acquired the benefit of eliminating contrast injection, which may be a significant issue in patients with renal impairment.

DWI has some benefits over DCE-MRI, including a shorter examination time. The procedure is also simple to repeat, allowing for close monitoring throughout the loco-regional treatment. DWI images also require less post-processing time than DCE-MRI images. Finally, in cases of tumor inhomogeneity, DWI is useful because it allows for a quick assessment of the entire tumor.

Limitation

In this study, some constraints were met. First, this prospective study had a small number of patients included; nevertheless, several other studies had a similar number of patients [1, 12, 13]. Second, technical issues

Elrefaey Hasan *et al. Egypt J Radiol Nucl Med*   (2021) 52:267

Page 11 of 12

Table 4 Diagnostic performance of DCE, DWI, ADC, normalized ADC liver and normalized ADC spleen

	DCE	DWI	ADC[a]	nADC liver[b]	nADC spleen[c]
Viable	15	15	12	13	14
Non-viable	25	25	28	28	26
TP	15	12	12	11	12
TN	25	22	25	24	23
FP	0	3	0	1	2
FN	0	3	3	4	3
Sensitivity	100%	80%	80%	73.3%	80%
Specificity	100%	88%	100%	96%	92%
PPV	100%	80%	100%	91.7%	85.7%
NPV	100%	88%	89.3%	85.7%	88.5%
Accuracy	100%	85%	97.1%	92.8%	91.9%

nADC normalized ADC, *TP* true positive, *TN* true negative, *FP* false positive, *FN* false negative

[a] ADC cutoff value less than (1.01×10^{-3} mm^2/s)

[b] normalized ADC liver cutoff value less than (0.81)

[c] normalized ADC spleen cutoff value less than (1.22)

with the DWI technique, such as respiratory and pulsation motion artifacts, particularly for peripherally placed lesions near the diaphragmatic copula, resulting in a low signal-to-noise ratio and a loss of spatial resolution. Partial volume averaging issues were also encountered, which resulted in calculation mistakes, and we attempted to overcome these challenges by using the lowest ROI feasible and taking numerous measurements.

Conclusions
The DWI and ADC map demonstrated excellent diagnostic performance for detecting post-RFA residual HCC, and it may be used in place of dynamic contrast-enhanced MRI in many cases where contrast administration is prohibited. Normalized ADC liver and normalized ADC spleen are additional parameters that can be used to enhance diagnostic value.

Abbreviations
HCC: Hepatocellular carcinoma; RFA: Radiofrequency ablation; MRI: Magnetic resonance imaging; DCE-MRI: Dynamic contrast-enhanced magnetic resonance imaging; DWI: Diffusion-weighted images; ADC: Apparent diffusion coefficient; T: Tesla; HFL: Hepatic focal lesion; LR-TR: LI-RADS treatment response; TSE: Turbo spin-echo; EPI: Echo-planar imaging; LAVA: Liver acquisition with volume acceleration; LI-RADS: Liver imaging reporting and data system; ROI: Region of interest; nADC: Normalized ADC; SPSS: Statistical package for the social sciences; PPV: Positive predictive value; NPV: Negative predictive value; ROC: Receiver operating characteristic; TACE: Trans-arterial chemoembolization; TP: True positive; TN: True negative; FP: False positive; FN: False negative.

Availability of data and materials
All the datasets used and analyzed in this study are available with the corresponding author on reasonable request.

Declarations

Ethics approval and consent to participate
Written informed consent was signed by all patients before the examination. The study was approved by the Research Ethics Committee (REC) of the Faculty of Medicine, Ain Shams University, FWA 00017585 (Approval Number R1/2016), and experiments were conducted in accordance with the ethical guidelines.

Consent for publication
All patients included in this research were fully conscious and older than 18 years old and gave written informed consent to publish the data contained within this study.

Competing interests
The authors declare that they have no competing interests.

Author details
[1] Radiology Department, Military Medical Academy, Cairo, Egypt. [2] Radiology Department, Faculty of Medicine, Ain Shams University, Cairo, Egypt.

References
1. Mahmoud BM, Elkholy SF, Nabeel MM, Abdelaziz AO, Elbaz T, Shoush HI, Ibrahim M, Hashem A, Ramadan AH, Abdelmaksoud AH (2016) Role of MRI in the assessment of treatment response after radiofrequency and microwave ablation therapy for hepatocellular carcinoma. Egypt J Radiol Nucl Med 47(2):377–385
2. Altekruse SF, McGlynn KA, Dickie LA, Kleiner DE (2012) Hepatocellular carcinoma confirmation, treatment, and survival in surveillance, epidemiology, and end results registries, 1992–2008. Hepatology 55(2):476–482
3. Curley SA, Izzo F, Ellis LM, Nicolas Vauthey J, Vallon P (2000) Radiofrequency ablation of hepatocellular cancer in 110 patients with cirrhosis. Ann Surg 232(3):381–391
4. Van Beers BE, Daire JL, Garteiser P (2015) New imaging techniques for liver diseases. J Hepatol 62(3):690–700
5. Kim KW, Lee JM, Choi BI (2010) Assessment of the treatment response of HCC. Abdom Imaging 36(3):300–314
6. Taouli B, Koh DM (2010) Diffusion-weighted MR imaging of the liver. Radiology 254(1):47–66
7. Saito K, Tajima Y, Harada TL (2016) Diffusion-weighted imaging of the liver: current applications. World J Radiol 8(11):857–867
8. Kielar A, Fowler KJ, Lewis S et al (2018) Locoregional therapies for hepatocellular carcinoma and the new LI-RADS treatment response algorithm. Abdom Radiol (NY) 43(1):218–230
9. Balogh J, Victor D 3rd, Asham EH et al (2016) Hepatocellular carcinoma: a review. J Hepatocell Carcinoma 3:41–53

Elrefaey Hasan *et al. Egypt J Radiol Nucl Med*　(2021) 52:267

Page 12 of 12

10. Yuan Z, Ye XD, Dong S, Xu LC, Xu XY, Liu SY, Xiao XS (2010) Role of magnetic resonance diffusion-weighted imaging in evaluating response after chemoembolization of hepatocelluler carcinoma. Eur J Radiol 75:e9-14

11. Granata V, Petrillo M, Fusco R, Setola SV, de Lutio di Castelguidone E, Catalano O, Piccirillo M, Albino V, Izzo F, Petrillo A (2013) Surveillance of HCC patients after liver RFA: role of MRI with hepato-specific contrast versus three-phase CT scan-experience of high volume oncologic institute. Gastroenterol Res Pract 2013:469

12. Ebeed AE, Romeih MA, Refat MM, Youssef MH (2017) Role of dynamic contrast-enhanced and diffusion weighted MRI in evaluation of hepatocellular carcinoma after chemoembolization. Egypt J Radiol Nucl Med 48:807–815

13. Saleh TY, Bahig S, Shebraya N et al (2019) Value of dynamic and DWI MRI in evaluation of HCC viability after TACE via LI-RADS v2018 diagnostic algorithm. Egypt J Radiol Nucl Med 50:113

14. Chernyak V, Fowler KJ, Kamaya AK et al (2018) liver imaging reporting and data system (LI-RADS) version 2018: imaging of hepatocellular carcinoma in at-risk patients. Radiology 289(3):816–830

15. Ludwig JM, Camacho JC, Kokabi N, Xing M, Kim HS (2015) The role of diffusion-weighted imaging (DWI) in locoregional therapy outcome prediction and response assessment for hepatocellular carcinoma (HCC): the new era of functional imaging biomarkers. Diagnostics (Basel) 5(4):546–563

16. Yousef MI, Refaat MM, Faheem MH (2017) role of diffusion-weighted magnetic resonance imaging in the evaluation of hepatocellular carcinoma response to transcatheter arterial chemoembolization using drug eluting beads; correlation with dynamic MRI. Egypt J Radiol Nucl Med 48(4):817–824

17. Yu JS, Kim JH, Chung JJ, Kim KW (2009) Added value of diffusion-weighted imaging in the MRI assessment of peri-lesional tumor recurrence after chemoembolization of hepatocellular carcinomas. J Magn Reson Imaging 30(1):153–160

18. Mostafa MMS (2016) Diffusion weighted and dynamic contrast enhanced magnetic resonance imaging in assessment of malignant liver tumors after percutaneous radiofrequency ablation. Egypt J Radiol Nucl Med 47:1195–1205

19. Nassef HH, Sheh AS, Radhi AA (2017) The role of diffusion weighted MR imaging in assessment of hepatocellular carcinoma after radiofrequency ablation. Egypt J Hosp Med 69(2):1908–1910

20. Schraml C, Schwenzer N, Clasen S, Rempp HJ, Martirosian P, Claussen CD, Pereira PL (2009) Navigator respiratory triggered diffusion weighted imaging in the follow up after hepatic radiofrequency ablation initial results. J Magn Reson Imaging 29(6):1308–1316

21. Barral M, Sebbag-Sfez D, Hoeffel C et al (2013) Characterization of focal pancreatic lesions using normalized apparent diffusion coefficient at 1.5-Tesla: preliminary experience. Diagn Interv Imaging 94(6):619–627

22. Abdelrahman AS, Ashour MMM, Abdelaziz TT (2020) Predictive value of neck imaging reporting and data system (NIRADS) in CECT/CEMRI of laryngeal and oral cavity squamous cell carcinoma. Egypt J Radiol Nucl Med 51:241

23. Abdelaziz TT, Abdel Razk AAK, Ashour MMM et al (2020) Interreader reproducibility of the neck imaging reporting and data system (NI-RADS) lexicon for the detection of residual/recurrent disease in treated head and neck squamous cell carcinoma (HNSCC). Cancer Imaging 20:61

24. Abdelrahman AS, Abdel-Rahman AS, Taha NM (2021) The role of functional imaging; DWI, ADC and 18F-FDG PET/CT in the evaluation of HCC treatment response after transarterial chemoembolization. Egypt J Radiol Nucl Med 52:217

Publisher's Note